DOT/FAA/AR-02/44

Office of Aviation Research
Washington, D.C. 20591

Combustibility of Cyanate Ester Resins

June 2002

Final Report

U.S. Department of Transportation
Federal Aviation Administration

NOTICE

This report is available at the Federal Aviation Administration William J. Hughes Technical Center's Full-Text Technical Reports page: actlibrary.tc.faa.gov in Adobe Acrobat portable document form (PDF).

Technical Report Documentation Page

1. Report No.	2. Government Accession No.	3. Recipient's Catalog No.
DOT/FAA/AR-02/44		

4. Title and Subtitle	5. Report Date
COMBUSTIBILITY OF CYANATE ESTER RESINS	June 2002
	6. Performing Organization Code

7. Author(s)	8. Performing Organization Report No.
Richard E. Lyon, Richard Walters* and S. Gandhi*	

9. Performing Organization Name and Address	10. Work Unit No. (TRAIS)
Federal Aviation Administration William J. Hughes Technical Center Airport and Aircraft Safety Research and Development Division Fire Safety Branch Atlantic City International Airport, NJ 08405 *Galaxy Scientific Corp. 2500 English Creek Ave., Bldg. C Egg Harbor Township, NJ 08234	11. Contract or Grant No.

12. Sponsoring Agency Name and Address	13. Type of Report and Period Covered
U.S. Department of Transportation Federal Aviation Administration Office of Aviation Research Washington, DC 20591	Final Report
	14. Sponsoring Agency Code AIR-120

15. Supplementary Notes

The FAA William J. Hughes Technical Center COTR is Richard Lyon.

16. Abstract

Flaming and nonflaming combustion studies were conducted on a series of polycyanurates to examine the effect of chemical composition and physical properties on the fire behavior of these cross-linked, char-forming thermoset polymers. Heats of complete combustion of the polymer and fuel gases were determined by oxygen bomb calorimetry and pyrolysis-combustion flow calorimetry, respectively. Fire calorimetry experiments were conducted to measure the heat released, the rate of heat release, and the smoke generation in flaming combustion. Fire response parameters derived from the data include the thermal inertia, heat of gasification, effective heat of combustion, and combustion efficiency. Halogen-containing polycyanurates exhibited extremely low heat release rate in flaming combustion compared to the hydrocarbon resins, yet produced significantly less smoke and comparable levels of carbon monoxide and soot.

17. Key Words	18. Distribution Statement
Polycyanurate, Cyanate ester, Fire, Flammability, Thermoset polymer	This document is available to the public through the National Technical Information Service (NTIS), Springfield, Virginia 22161.

19. Security Classif. (of this report)	20. Security Classif. (of this page)	21. No. of Pages	22. Price
Unclassified	Unclassified	26	

TABLE OF CONTENTS

LIST OF FIGURES

LIST OF TABLES

EXECUTIVE SUMMARY

Flaming and nonflaming combustion studies were conducted on a series of polycyanurates to examine the effect of chemical composition and physical properties on the fire behavior of these cross-linked, char-forming thermoset polymers. Heats of complete combustion of the polymer and fuel gases were determined by oxygen bomb calorimetry and pyrolysis-combustion flow calorimetry, respectively. Fire calorimetry experiments were conducted to measure the heat released, the rate of heat release, and the smoke generation in flaming combustion. Fire response parameters derived from the data include the thermal inertia, heat of gasification, effective heat of combustion, and combustion efficiency. Halogen-containing polycyanurates exhibited extremely low heat release rate in flaming combustion compared to the hydrocarbon resins, yet produced significantly less smoke and comparable levels of carbon monoxide and soot.

INTRODUCTION

Polycyanurates are thermoset polymers that are cross-linked through the cyclotrimerization reaction of three cyanate ester (–O–C≡N) groups to form oxygen-linked triazine rings (cyanurates). Polymerization (curing) occurs via a thermally-activated addition reaction which produces no volatiles, so that void-free castings and fiber reinforced composites with good surface finish can be obtained. The chemistry and properties [1], flammability [2], and fire behavior [3-6] of cyanate esters have been reviewed in detail. Recent work by the Federal Aviation Administration (FAA) [7] shows that aromatic polycyanurates thermally decompose by a common mechanism which begins with thermolytic cleavage of the resin backbone between 300°–450°C, and culminates with decyclization of the cyanurate rings, at 450° ±8°C, to produce a variety of volatile fuel species as shown schematically in figure 1. The amount of char formed in the thermal degradation process ranges from 30% to 60% in rough proportion to the aromatic content of the polycyanurate backbone. The char contains carbon, hydrogen, nitrogen, and oxygen in the approximate atomic ratio C/H/O/N = 15/4/2/1 as indicated in figure 1. Because the thermal decomposition (ignition) temperature and heat transport properties of the polycyanurates are relatively independent of the backbone, chemical structure, the fire behavior of these materials will depend only on their fuel value, char yield, and char properties. The present flaming and nonflaming combustion studies are an attempt to correlate the fire behavior of polycyanurates with their chemical structure.

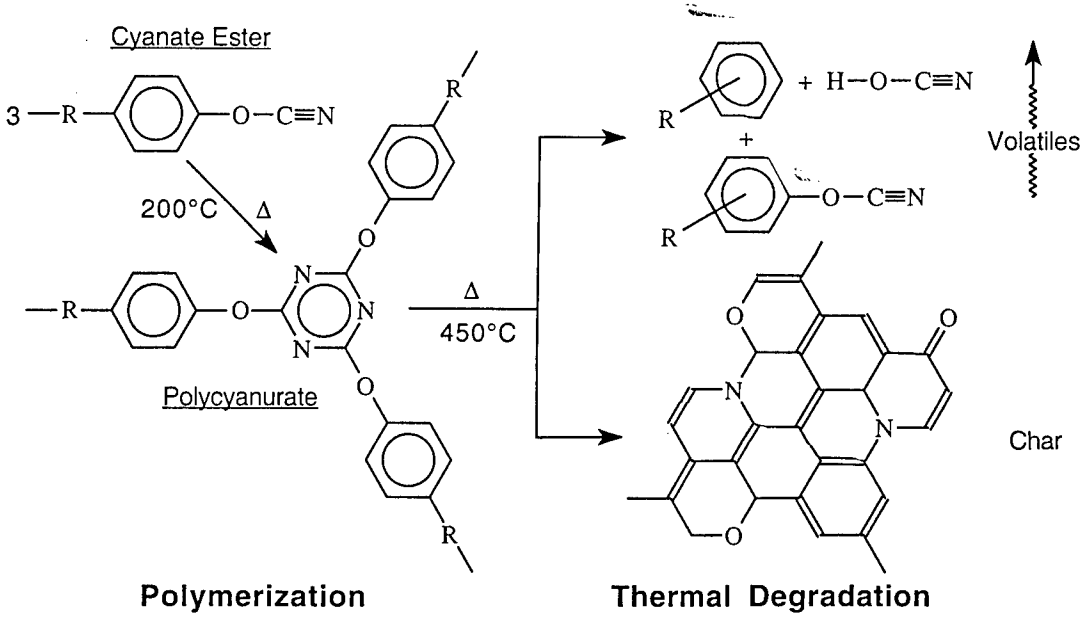

FIGURE 1. CYANATE ESTER POLYMERIZATION AND THERMAL DEGRADATION REACTIONS

EXPERIMENTAL

MATERIALS.

A list of the cyanate ester monomers along with their trade name, atomic formula, and chemical structure are shown in table 1. The cyanate ester resins AroCy B-10, L-10, F-10, M-10, XU-366,

XU-371, XU-71787.02L, and RD98-228 were produced by Ciba Specialty Chemicals, Performance Polymers Division, Brewster, NY (currently Vantico). The phenol novolac-based cyanate ester resins Primaset PT-30, PT-60, and PT-90 are produced by Lonza Incorporated, Fairlawn, NJ. Cured plaques of resin XU-71787.02L were provided by Y.L.A. Incorporated, Benecia, CA. All of the cyanate ester monomers in this study were one-part, 100% solids, commercial (or precommercial) samples which were used as received without further purification or catalysts.

TABLE 1. TRADE NAMES AND CHEMICAL STRUCTURE OF THE CYANATE ESTER MONOMERS

Trade Name	Chemical Designation [CAS Reg. No.]	Formula	Structure
AroCy B-10	Bisphenol-A Cyanate Ester [1156-51-0]	$C_{17}H_{14}O_2N_2$	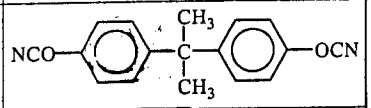
AroCy F-10	Hexafluorobisphenol-A Cyanate Ester [32728-27-1]	$C_{17}H_8O_2N_2F_6$	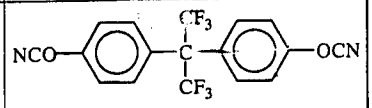
AroCy L-10	Bisphenol-E Cyanate Ester [47073-92-7]	$C_{16}H_{12}O_2N_2$	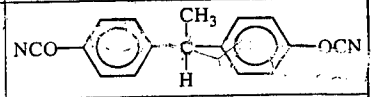
AroCy M-10	Tetramethylbisphenol-F Cyanate Ester [107657-77-6]	$C_{19}H_{18}O_2N_2$	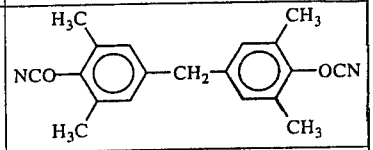
AroCy XU-366	Bisphenol-M Cyanate Ester [127667-44-1]	$C_{26}H_{24}O_2N_2$	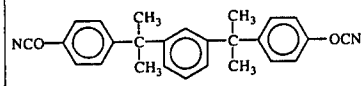
AroCy XU-371	Phenol Novolac Cyanate Ester [P88-1591]	$C_{23}H_{15}O_3N_3$	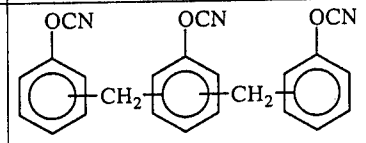
AroCy RD98-228	Bisphenol-C Cyanate Ester BPC = [14868-03-2]	$C_{16}H_8N_2O_2Cl_2$	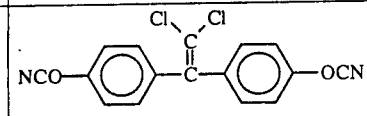
AroCy XU-71787.02L	Dicyclopentadienyl-bisphenol Cyanate Ester [119505-06-5]	$C_{17}H_{17}NO$	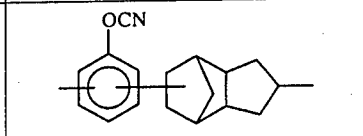
Primaset PT-30 PT-60 PT-90	Novolac Cyanate Ester n = 1 [Ass. No. 160817] n = 4 [Ass. No. 160817] n = 7 [153191-90-3]	$C_{23}H_{15}O_3N_3$ $C_{47}H_{30}N_6O_6$ $C_{71}H_{45}N_9O_9$	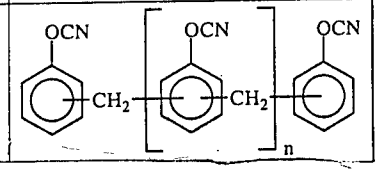

Samples for oxygen bomb calorimetry, fire (cone) calorimetry, pyrolysis-combustion flow calorimetry (PCFC), and thermogravimetric analysis (TGA) were made by pouring the warmed (50°C) liquid resins into Teflon-coated aluminum molds, degassing under vacuum at 50°C, and then curing in a convection oven for 18 hours at 150°C, 4 hours at 200°C, and 4 hours at 250°C. The solid samples were then cooled to room temperature, removed from the mold, and postcured free-standing at 300°C for an additional 15 minutes. The fully cured samples were 10- x 10- x 0.64-cm solid plaques that were semitransparent and amber or dark brown in color. These polycyanurate samples were used directly for fire calorimetry or cut into samples for oxygen bomb calorimetry, PCFC, and TGA. Methane, oxygen, and nitrogen gases used for calibration and testing were dry, >99.99% purity grades obtained from Matheson Gas Products.

METHODS.

OXYGEN BOMB CALORIMETRY. Values for the gross heat of combustion were obtained with an oxygen bomb calorimeter (Parr Instrument Model 1341) using the American Society for Testing and Materials (ASTM) standard test method D 2382-88 [8]. Approximately 1 gram of sample is placed inside a sample cup in a pressure vessel (oxygen bomb) which is in contact with an ignition wire connected to two electrodes. The bomb is then sealed, purged, and pressurized to 20 atmospheres with pure oxygen. The sealed bomb is then placed inside a 2-liter water bath which is inside an adiabatic container. Upon thermal equilibration of the system at ambient temperature, the sample is ignited and completely combusted. The gross heat of combustion of the sample at room temperature is calculated from the temperature rise of the water bath ΔT (°K), which is typically a few degrees Kelvin, the calibration factor C (J/°K), and the initial mass m_0 (g) according to

$$h^0_{c,s}(\text{gross}) = (C\Delta T - c_1 - c_2)/m_0 \qquad (1)$$

where c_1 and c_2 are the correction factors for the heat of combustion of the ignition wire and the heat of formation of acids, respectively, in units of kJ. The net heat of complete combustion $h^0_{c,s}(\text{net})$ is calculated from the gross heat of complete combustion in kJ/g according to equation 2. [9]

$$h^0_{c,s}(\text{net}) = h^0_{c,s}(\text{gross}) - (w_H)(21.96\ \text{kJ/g}) \qquad (2)$$

where w_H is the weight fraction of hydrogen in the sample. The net heat of combustion accounts for the fact that at fire temperatures (≈ 1000°C), water is in the gaseous state so that its heat of vaporization/condensation must be subtracted from the gross (room temperature) heat of combustion.

PYROLYSIS COMBUSTION FLOW CALORIMETRY. Specific heat release, Q_c (J/g), and heat release rate (HRR), $\dot{Q}_c$(W/g), were measured in a PCFC developed by the FAA [10] for studying the molecular-level fire response of materials. A sample weighing 1.0 ±0.1 mg is heated in a nitrogen stream at 4K/s to force anaerobic pyrolysis at heating rates comparable to those at a solid surface during steady flaming combustion. The volatile decomposition products are purged to a high temperature (900°C) combustion furnace, where oxygen is added to effect complete (nonflaming) combustion of the volatile fuel. Carbon dioxide, water, and (if necessary)

acid gases are removed from the sample stream using Drierite™ and Ascarite™ scrubbers. According to the principle of oxygen consumption calorimetry [11 and 12], the amount of heat liberated by complete combustion of typical hydrocarbon fuels is proportional to the mass of oxygen consumed in the oxidation reactions. The empirical proportionality constant E = 13.1 ±0.6 kJ/g-O_2 is the amount of heat liberated on average per gram of diatomic oxygen consumed by combustion. Therefore, the rate of heat released by combustion of the pyrolysis (fuel) gases in the PCFC is $E\Delta\dot{m}_{O_2} = h^0_{c,v}\,\dot{m}_s$, where $\dot{m}_s$, is the mass loss rate of the pyrolyzing solid sample and $h^0_{c,v}(t)$ is the instantaneous net heat of complete combustion of the volatile pyrolysis products per unit mass. Dividing the heat release rate by the initial sample weight m_o gives the specific heat release rate $\dot{Q}_c$ in units of W/g.

$$\dot{Q}_c(t) = \frac{E}{m_0}\Delta\dot{m}_{O_2}(t) = \frac{h^0_{c,v}(t)}{m_0}\dot{m}_s(t) \tag{3}$$

The total heat, Q_c, released by combustion per unit initial mass of solid is obtained from equation 3 as the time integral of the oxygen consumption rate after the experiment when the baseline returns to zero ($t = \infty$)

$$Q_c = \frac{E}{m_0}\int_0^\infty \Delta\dot{m}_{O_2}(t)\,dt = \frac{1}{m_0}\int_0^\infty h^0_{c,v}(t)\,\dot{m}_s(t)\,dt \tag{4}$$

It has been shown [10] that the maximum value of the specific heat release rate measured in the PCFC has an analytic form in a constant heating rate experiment

$$\dot{Q}_c^{max} = \frac{E}{m_0}\Delta\dot{m}_{O_2}^{max} = h^0_{c,v}\left(\frac{\dot{m}_s^{max}}{m_0}\right) = h^0_{c,v}\frac{\beta E_a(1-\mu)}{eRT_p^2} \tag{5}$$

where β (K/s) is the constant heating rate, E_a (J/mole-K) is the global activation energy for pyrolysis, μ (g/g) is the char fraction, e is the natural number, R is the gas constant, and T_p (K) is the temperature at maximum mass loss rate, $\dot{m}_s^{max}$(g/s). Dividing equation 5 by β yields a derived quantity containing only material properties and having the units (J/g-K) and significance of a heat (release) capacity.

$$\eta_c = \frac{\dot{Q}_c^{max}}{\beta} = h^0_{c,v}\frac{(1-\mu)E_a}{eRT_p^2} \tag{6}$$

The heat release capacity η_c as measured, for example, in the PCFC, is a molecular level fire property that is proportional to the heat release rate per unit area in steady flaming combustion [13] and is calculable from additive molar group contributions [14].

FIRE CALORIMETRY. The HRR, mass loss rate (MLR), smoke density, and combustion gases were measured in a fire calorimeter (Cone2a, Atlas Electric) operating on the oxygen

consumption principle according to ASTM E1354 [15], as described in detail by Babrauskas [16]. The cold wall external radiant heat flux was set at 35, 50, 75, and 100 kW/m^2 using a Schmidt-Boelter heat flux gage. A spark igniter located 2.5 cm above the sample surface was kept in place until stable flaming combustion was observed. The smoke extinction coefficient k (1/m) was calculated from attenuation of the He-Ne laser beam intensity (I/I_0) over path length L (m) in the exhaust duct as, $k = (1/L) \ln (I/I_0)$.

Square samples (100 x 100 x 6.4 mm) of each material were tested in a horizontal orientation with the retainer edge frame, as per ASTM E1354 [15], for materials with tendency for swelling. The time to sustained ignition (t_{ig}), HRR, total heat release (THR), MLR, and effective heat of combustion (EHC) were measured for each material at each external irradiance level.

Yields of carbon monoxide and carbon dioxide per unit mass loss during flaming combustion (kg-CO_x/kg-mass loss) were calculated from the instantaneous mass flow rates of the gases (kg/s) divided by the sample mass loss rate $\dot{m}_s$(kg/s). Specific smoke extinction area (SEA) (m^2/kg), is calculated during the test from the volumetric flow rate in the exhaust duct V_f (m^3/s), the extinction coefficient k (1/m), and mass loss rate of the sample as $SEA = kV_f / \dot{m}_s$. Extinction area is related to the number and size of smoke particles produced, with higher extinction area causing greater attenuation of the laser beam intensity in the test and, in principle, greater obscuration in a fire. Instantaneous smoke production rate (SPR), (m^2/s), is calculated as the product of the extinction coefficient and the volumetric flow rate in the exhaust duct divided by the sample surface area A, $SPR = kV_f/A$. The smoke production rate, like the mass loss rate, tends to track the heat release rate fairly closely. The mass of soot generated per unit mass of burned sample (kg/kg) was measured for the entire duration of the test by diverting 0.2% of the exhaust duct flow through a 47-mm-diameter microfiberglass collection filter (Whatman #1820047) using a mass flow controller and weighing the filter before and after the test.

RESULTS AND DISCUSSION

NONFLAMING COMBUSTION.

The gross and net heats of complete combustion of the polycyanurates from oxygen bomb calorimetry are listed in table 2. Excluding the halogen-containing polymers, F-10 and RD98-228, the net heats of combustion fall within the relatively narrow range 28.6-34.4 kJ/g. The net heat of complete combustion of the polycyanurate $h^0_{c,p}$ is, on average, about 20% greater than the net heat of combustion of the volatile degradation products, $h^0_{c,v}$, determined by pyrolysis combustion flow calorimetry. The disparity between the heats of combustion of the polymer and its fuel gases is the result of partitioning of degradation products into nitrogen (N) and oxygen (O) enriched volatile fuel and N, O depleted carbonaceous char during thermal degradation (see figure 1). The heat of combustion of the volatile fuel gases $h^0_{c,v}$ is related to the heat of combustion of the polymer $h^0_{c,p}$ and its char $h^0_{c,\mu}$ as

$$h^0_{c,v} = \frac{h^0_{c,p} - \mu h^0_{c,\mu}}{1 - \mu} \qquad (7)$$

The last column of table 2 are the net heats of complete combustion of the char calculated with equation 7 from $h^{o}_{c,p}$, $h^{o}_{c,v}$, and μ for each polycyanurate. It is seen that $h^{o}_{c,\mu}$ increases with the carbon/hydrogen content of the polymer (see table 1). The char fraction or pyrolysis residue increases from 27% to 65% in rough proportion to the aromatic content of the monomer backbone as predicted from group contributions to the char forming tendency of polymers [17]. The pyrolysis residue is in reasonable agreement with the char yield after flaming combustion measured in the cone calorimeter (compare table 4).

TABLE 2. NET HEAT OF COMPLETE COMBUSTION, SPECIFIC HEAT RELEASE, HEAT RELEASE CAPACITY, AND CHAR FRACTION FOR POLYCYANURATES

	Oxygen Bomb		PCFC				Calculated
Material	$h^{o}_{c,p}$(gross) kJ/g	$h^{o}_{c,p}$(net) kJ/g	Q_c kJ/g	η_c J/g-K	Char Fraction	$h^{o}_{c,v}$ kJ/g	$h^{o}_{c,\mu}$ kJ/g
B-10	29.92	28.81	17.6	283	0.36	27.6	31.0
F-10	18.71	18.25	4.6	62	0.43	8.1	31.7
L-10	29.38	28.38	14.7	316	0.42	25.3	32.6
M-10	31.23	29.94	17.4	280	0.35	26.9	35.1
XU-366	34.39	33.06	22.5	239	0.26	30.6	39.4
XU-371	28.76	27.77	9.1	88	0.59	21.9	31.9
XU-71787	33.64	32.14	20.1	493	0.27	27.6	43.6
PT-30	30.65	29.81	9.9	122	0.52	20.6	38.0
RD98-228	22.25	21.72	4.2	24	0.53	9.0	33.0

Figure 2 shows specific heat release rate data for the polycyanurates obtained in the pyrolysis-combustion flow calorimeter. The data have been horizontally shifted from the reference XU-71787 data in 200-second increments for clarity. The maximum value of the heat release rate for each polycyanurate was divided by the sample heating rate (4.3 K/s) to compute the heat release capacity listed in table 2 along with the total heat release (area under the curve) and the char residue after the test. Polycyanurates with the highest heat release capacity and total heat release (XU-71787 and XU-366) had the highest aliphatic hydrocarbon content and fuel value. Increasing aromatic hydrocarbon content over the series B-10, L-10, M-10, PT, and XU-371 resulted in increased char yield, lower heat release capacity, and lower total heat release in accordance with equations 4 and 5. The halogen-containing polycyanurates F-10 and RD98-228 exhibit high char yield and low heat of combustion of the fuel gases $h^{o}_{c,v}$ and therefore (see equation 6) had the lowest heat release capacity and total heat release.

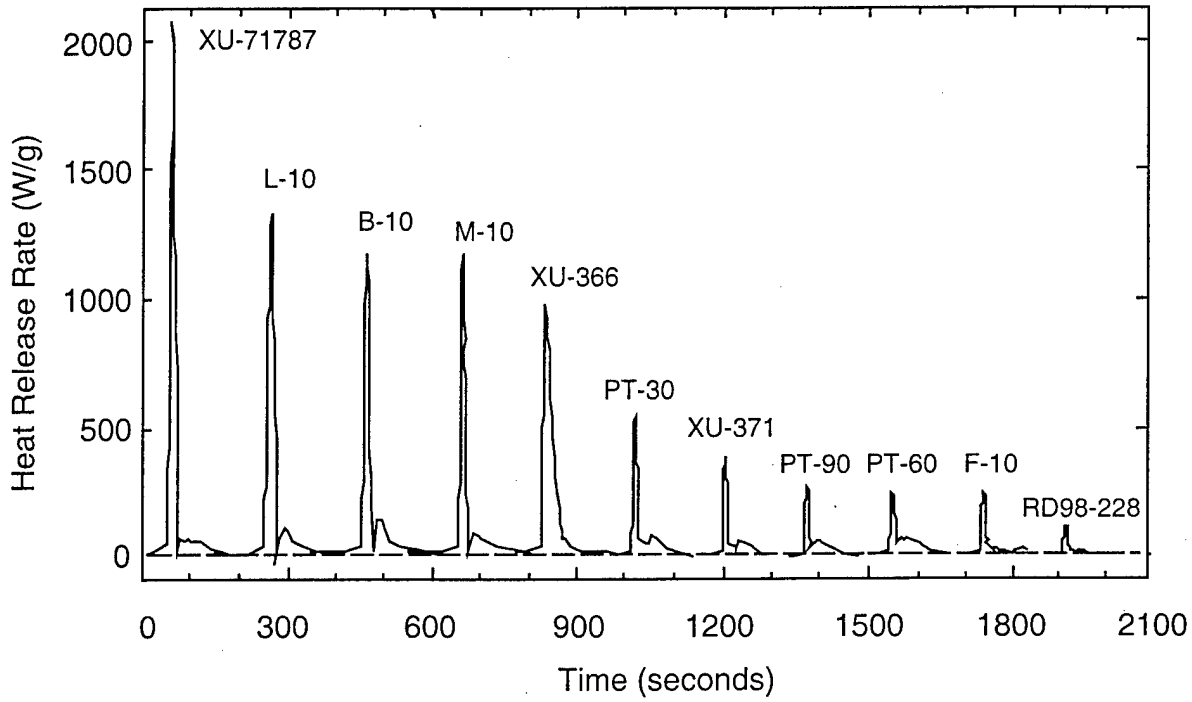

FIGURE 2. PYROLYSIS-COMBUSTION DATA FOR POLYCYANURATES
(Horizontally shifted for clarity)

FLAMING COMBUSTION.

Complete heat release rate histories for all of the polymers and heat fluxes tested are contained in appendix A. Table 3 lists flaming combustion parameters extracted from the data in the appendix for the polycyanurates. Listed in table 3 are the time-to-ignition (t_{ign}), the maximum heat release rate at ignition, i.e., the first peak in the HRR curves (HRR_{pk}), the average heat release rate (HRR_{av}) and the total heat released (THR) over the entire 20-minute duration of the test, the peak mass loss rate (MLR_{pk}), and the effective heat of combustion (EHC) at each of the incident heat fluxes. The heat of gasification per unit mass of volatile fuel (L_g), see column 8 of table 3, is obtained from the reciprocal slope of a plot of peak mass loss rate versus external heat flux. Values of L_g in parentheses are the result of only two peak mass loss rate, heat flux data pairs in table 3.

During the cone calorimeter tests, the exposed face of the material began gasifying soon after exposure to the radiant heat flux. Ignition of gaseous fuel emerging from the exposed surface occurred 1-2 minutes into the test followed by surface charring, char cracking, and the development of porosity. The times to ignition for the polycyanurates were comparable at a particular heat flux with the exception of the halogenated F-10 and RD98-228 cyanate esters which were significantly longer. In the case of the fluorinated polycyanurate F-10, there was no sustained ignition at 35 or 50 kW/m^2.

TABLE 3. FIRE BEHAVIOR OF POLYCYANURATES IN CONE CALORIMETER

Material	Heat Flux (kW/m^2)	t_{ig} (s)	HRR_{pk} (kW/m^2)	HRR_{av} (kW/m^2)	THR (MJ/m^2)	MLR_{pk} (g/m^2-s)	L_g (MJ/kg)	EHC (MJ/kg)
B10	35	171	166	92	93	8.3	4.0	25.5
	50	98	195	111	118	11.4		26.0
	75	40	246	157	160	22.3		27.5
	100	26	272	150	101	28.2		24.6
F10	35	NI	—	—	—	—	(3.0)	—
	50	(90)	—	—	—	—		—
	75	41	53	60	82	16.8		16.9
	100	27	78	45	53	25.2		9.8
L10	35	151	96	65	56	7.3	5.1	20.2
	50	88	149	104	102	10.3		26.0
	75	40	183	139	126	17.5		25.9
	100	22	204	145	100	19.6		24.1
M10	35	159	305	117	97	18.7	3.5	26.9
	50	69	251	125	117	10.0		27.1
	75	24	280	169	133	17.6		24.3
	100	19	338	173	112	35.5		25.1
PT30	35	202	179	71	46	19.8	5.0	19.1
	50	96	166	88	78	27.6		21.7
	75	40	118	112	83	34.8		21.2
	100	19	138	126	74	35.1		20.2
XU366	35	—	—	—	—	—	(2.2)	—
	50	69	202	149	152	11.0		28.4
	75	32	279	229	186	22.5		29.3
	100	—	—	—	—	—		—
XU371	35	203	204	68	42	20.9	(2.9)	17.5
	50	93	210	99	83	26.0		20.6
	75	41	231	123	79	27.0		20.9
	100	23	248	127	76	27.0		21.4
XU71787	35	167	244	55	51	12.98	4.4	24.9
	50	67	304	113	96	16.23		28.2
	75	32	378	172	165	24.6		28.6
	100	20	415	166	126	26.8		27.7
RD98-228	35	294	57	19	5.4	20	5.3	3.1
	50	189	124	45	13	17.6		3.5
	75	139	177	67	16	20.7		4.0
	100	129	186	57	19	32		4.1

IGNITABILITY. According to the thermal (heat transfer limited) theory of ignition, the time-to-ignition (t_{ign}) for a semi-infinite thickness of material having ignition temperature T_{ign} experiencing a net heat flux $\dot{q}_{net}$ is

$$t_{ign} = \frac{\pi}{4} k\rho c \left[\frac{T_{ign} - T_0}{\dot{q}_{net}} \right]^2 \tag{8}$$

where k, ρ, and c are the thermal conductivity, density, and heat capacity of the material, respectively. The net heat flux, $\dot{q}_{net}$, is equal to the external radiant heat flux, $\dot{q}_{ext}$, minus the heat lost to the environment at temperature T_0 by reradiation and convection, $\dot{q}_{loss}$, i.e.,

$$\dot{q}_{net} = \dot{q}_{ext} - \dot{q}_{loss} \tag{9}$$

In practice, the ignition time is found to depend on the ventilation conditions, ignition source, heat of combustion of the fuel value of the gases, etc. From equations 8 and 9

$$\frac{1}{\sqrt{t_{ign}}} = \frac{-\dot{q}_{loss}}{\sqrt{\frac{\pi k\rho c}{4}\left(T_{ign} - T_0\right)}} + \frac{\dot{q}_{ext}}{\sqrt{\frac{\pi k\rho c}{4}\left(T_{ign} - T_0\right)}} \tag{10}$$

Equation 10 applies if $L > 2(\alpha t_{ign})^{1/2}$, where L is the sample thickness and $\alpha = k/\rho c$ is the thermal diffusivity. In the present study L = 6.4 mm and $\alpha = 10^{-7}$ m^2/s (typically), so ignition times, $t_{ign} \leq L^2/4\alpha \approx 2$ minutes, are valid for use with equation 10. Thus, fire calorimeter data for time-to-ignition for the polycyanurates at the higher external heat fluxes can be analyzed to extract an average value of the product kρc that represents the thermal resistance (inertia) of a material to external heating over the temperature range from ambient to ignition. Figure 3 is the ignition data from table 3 for the B-10 polycyanurate plotted according to equation 10. The reciprocal slope of the line in figure 3 equals $(T_{ign}-T_0)(\pi k\rho c/4)^{1/2} = (\pi/4)^{1/2}$ TRP, where TRP = $(T_{ign}-T_0)(k\rho c)^{1/2}$ is referred to as the thermal response parameter (TRP). Values have been tabulated for many common polymers and composites [18]. If the ignition temperatures of the polycyanurates are equal to their decomposition temperatures, measured in laboratory thermogravimetric analyses [7], then kρc can be computed from the measured TRP. Table 4 lists the measured TRP and ignition (onset decomposition) temperature for each of the polycyanurates along with the thermal inertia (kρc) calculated from these data. The TRP values are at the high end of the range reported for common polymers 200–700 kW-s$^{1/2}$-m^{-2} [18] because of the relatively high decomposition temperature of the polycyanurates [7]. However, when T_{ign} is accounted for in the calculation of the thermal inertia, most of the kρc values of the polycyanurates are in the range of common, unfilled polymers, $k\rho c \approx 1.0 \pm 0.2$ kJ^2/m^4-s-K^4 [19]. The exceptions are the halogen-containing polycyanurates F-10 and RD98-228 which should have similar thermal properties to the other polycyanurates but instead exhibit experimental kρc values that are significantly higher, perhaps due to gas phase combustion inhibition not considered in the thermal (heat transfer limited) criterion for ignition (i.e., equation 10).

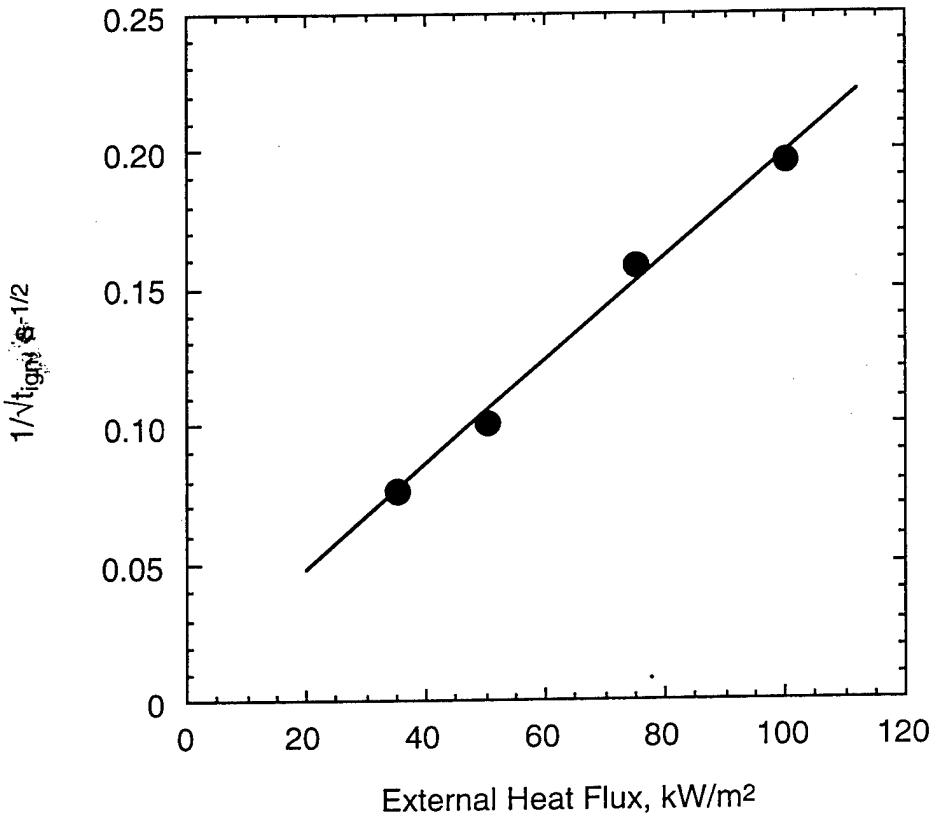

FIGURE 3. TIME-TO-IGNITION DATA FOR B-10 POLYCYANURATE

TABLE 4. IGNITION PROPERTIES OF POLYCYANURATES

Material	T_{ign}	TRP	kρc
	°C	kW-s$^{1/2}$/m^2	kJ^2/m^4-s-K^4
B-10	468	596	1.8
F-10	465	649	2.2
L-10	479	553	1.5
M-10	471	469	1.1
PT-30	462	463	1.1
XU-366	482	500	1.2
XU-371	461	531	1.5
XU-7178	463	508	1.3
RD98-228	461	705	2.6

HEAT RELEASE RATE. Figure 4 shows heat release rate histories for all of the polycyanurates at an external flux of 50 kW/m^2, with the exception of F-10 which did not sustain burning at that flux. The heat release rate curves are vertically shifted for clarity. The top four curves shown in figure 4 are data for the polycyanurates of monomers containing more than two reactive cyanate ester groups (i.e., functionality, f > 2) PT-30/60/90 and XU-371. These f > 2 polycyanurates showed an initial peak in heat release rate at ignition followed by a decrease in HRR as the char

layer forms and increases in thickness preventing the escape of pyrolysis (fuel) gases generated below the surface. A second heat release rate peak is observed for f > 2 polycyanurates about a minute after the ignition peak that corresponds to a catastrophic fracture of the charred surface and the instantaneous release of pressurized pyrolysis gases formed at depth [20].

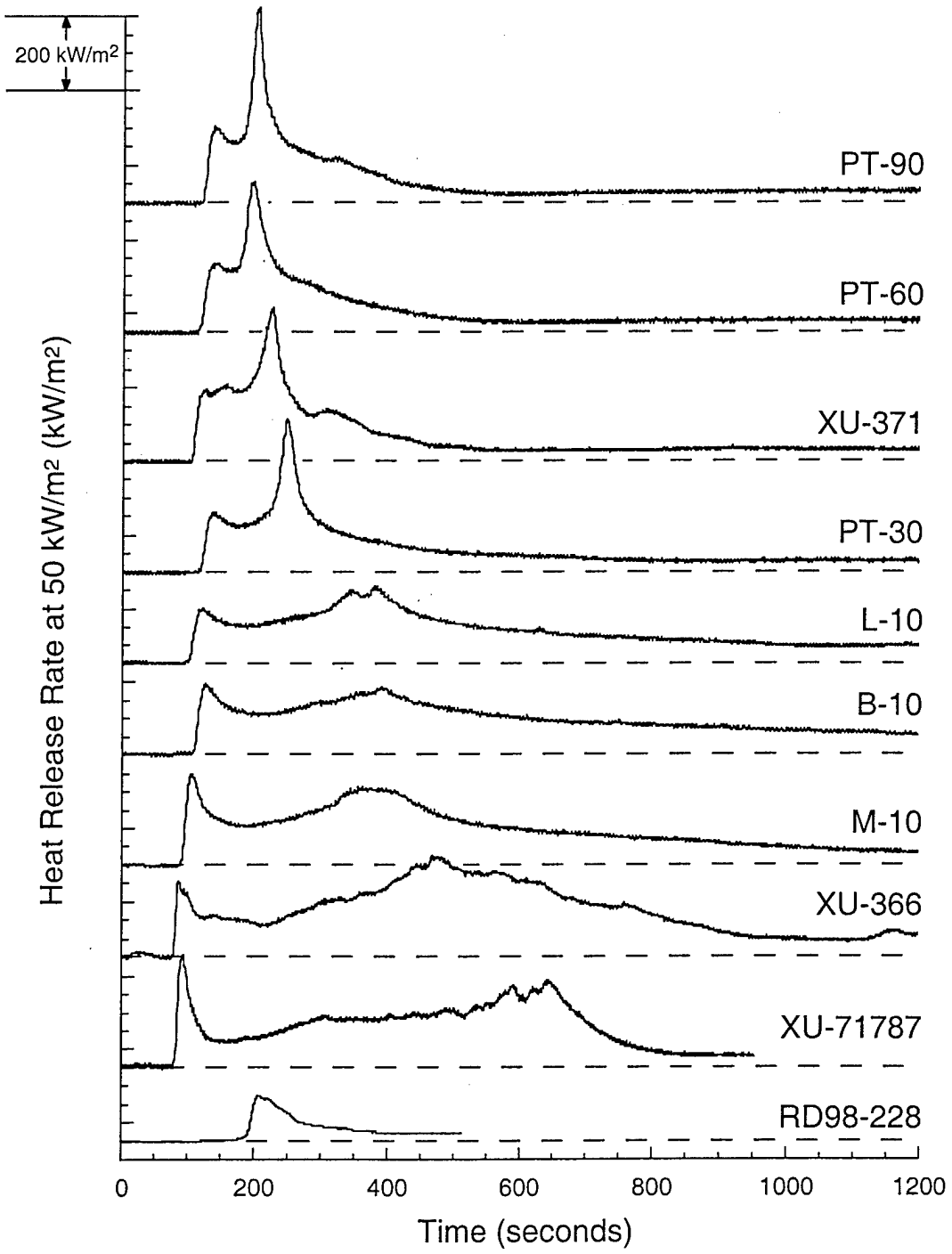

FIGURE 4. HEAT RELEASE RATE HISTORIES OF POLYCYANURATES AT 50 kW/m^2 HEAT FLUX IN CONE CALORIMETER

The heat release rate histories of the polycyanurates of the difunctional (f = 2) cyanate ester monomers L-10, B-10, M-10, XU-366, XU-71787, and RD98-228 are the lower six curves in figure 4. These f = 2 polycyanurates show the same initial heat release rate peak at ignition as does the polycyanurates from the f > 2 monomers. However, with the exception of RD98-228, the secondary heat release rate peak is broad and lower than the peak at ignition and occurs much later in the heat release history. The broad secondary HRR peak of the f = 2 polycyanurates corresponds to char swelling and the generation of numerous small fissures in the char surface that gradually release the pyrolysis gases formed at depth. The absence of catastrophic char fracture during the burning of polycyanurates from f = 2 monomers may be due to their lower char yield (35 ±7%) compared to the multifunctional resins (56 ±5%) and/or greater char permeability to pyrolysis gases. The f > 2 polycyanurates have a lower molecular weight between cyanurate rings (higher cross-link density) [17] than those from f = 2 resins, which could explain their higher char yield and the brittle fracture of their char during burning.

Solid materials generate gaseous fuel when the total heat absorbed by the solid is sufficient to raise the temperature of the material to the thermal decomposition temperature (latent heat), break primary chemical bonds in the polymer to make fuel fragments, and vaporize the resulting fuel fragments. This is the heat of gasification per unit mass of solid polymer, h_g. The heat of gasification determined from mass loss rate measurements, L_g in table 3, is the heat per unit mass of volatile fuel and it is obtained as the reciprocal slope of a plot of the peak mass loss rate ($\dot{m}''$) versus external heat flux ($\dot{q}''_{ext}$) assuming

$$\dot{m}'' = \frac{\dot{q}_n}{L_g} = \frac{\dot{q}_{ext} + \dot{q}_{fl} - \dot{q}_{rr}}{L_g} \qquad (11)$$

where $\dot{q}''_{fl}$ is the flame heat flux back to the surface and $\dot{q}''_{rr}$ is the heat lost from the surface due to reradiation. The char yields μ and L_g in table 3 can be used to calculate the heat of gasification per unit mass of polycyanurate, $h_g = (1-\mu)L_g = 2.5 \pm 0.7$ kJ/g, typical of synthetic polymers [21]. The narrow range of h_g indicates that the latent heats, bond breaking energies, and heats of vaporization of the degradation products that comprise h_g are similar for these polycyanurates, as would be expected based on their similar chemical composition and thermal degradation temperature.

COMBUSTION PRODUCTS. Table 5 lists data at 35, 50, 75, and 100 kW/m^2 radiant heat flux for the products of flaming combustion, i.e., the smoke yield in terms of specific extinction area, carbon monoxide (CO) and carbon dioxide (CO_2) yields, soot yield, and the residual mass (char) fraction after the test. The combustion efficiency in the flame χ is calculated as the ratio of the effective heat of flaming combustion (EHC in table 3) to the heat of complete combustion of the fuel gases ($h^0_{c,v}$ in table 2), i.e., $\chi = EHC/h^0_{c,v}$. The reported values for the combustion efficiency and combustion products are cumulative values for the entire test duration. Product yields are per unit mass of sample consumed. Char yield is expressed per unit initial mass of sample. The data in table 4 (with the exception of F-10) for soot yield, CO, and CO_2 (the latter quantities expressed as the ratio CO/CO_2) are plotted versus combustion efficiency in figure 5.

TABLE 5. CONE CALORIMETER DATA FOR SMOKE OBSCURATION AND COMBUSTION PRODUCTS YIELDS

Material	Heat Flux kW/m^2	SEA m^2/kg	CO kg/kg	CO_2 kg/kg	Soot Yield kg/kg	Combustion Efficiency, χ	Char % w/w
B10	35	583.7	0.01	1.87	0.087	0.92	48.7
	50	440.5	0.10	1.78	0.071	0.94	24.8
	75	683.2	0.04	2.20	0.085	1.00	19.1
	100	783.2	0.02	1.94	0.110	0.89	22.5
F10	75	54.6	0.14	1.91	0.041	2.1	16.0
	100	77.8	0.03	1.15	0.033	1.2	32.7
L10	35	522.9	0.04	1.65	0.055	0.80	61.5
	50	452.5	0.15	1.98	0.035	1.03	33.0
	75	540.6	0.08	2.10	0.078	1.02	27.0
	100	705.2	0.02	1.80	0.100	0.95	30.2
M10	35	723.6	0.07	1.84	0.077	1.00	53.3
	50	709.6	0.00	0.00	0.065	1.01	29.0
	75	771.3	0.02	1.61	0.092	0.90	23.6
	100	924.3	0.03	1.71	0.173	0.93	35.4
PT30	35	312.8	0.01	0.96	0.033	0.93	70.2
	50	235.9	0.05	1.61	0.040	1.05	56.9
	75	320.7	0.01	1.58	0.040	1.03	53.2
	100	395.6	0.01	1.49	0.047	0.98	50.5
XU371	35	345.7	0.00	0.91	0.038	0.80	70.3
	50	233.3	0.04	1.59	0.039	0.94	53.8
	75	305.7	0.00	0.00	0.039	0.95	54.8
	100	353.6	0.01	1.41	0.039	0.98	50.8
XU366	50	960.1	0.17	1.93	0.170	0.93	20.9
	75	906.6	0.12	2.04	0.134	0.96	17.0
XU71787	35	863.17	0.033	1.86	0.162	0.90	73
	50	747.72	0.024	1.93	0.123	1.02	58
	75	627.32	0.052	2.07	0.10	1.04	28
	100	767.72	0.02	1.85	0.11	1.00	43
RD98-228	35	123.0	0.039	0.240	0.030	0.34	62.0
	50	70.0	0.036	0.426	0.036	0.39	46.0
	75	97.0	0.036	0.376	0.030	0.44	55.0
	100	222.3	0.025	0.250	0.027	0.46	48.8

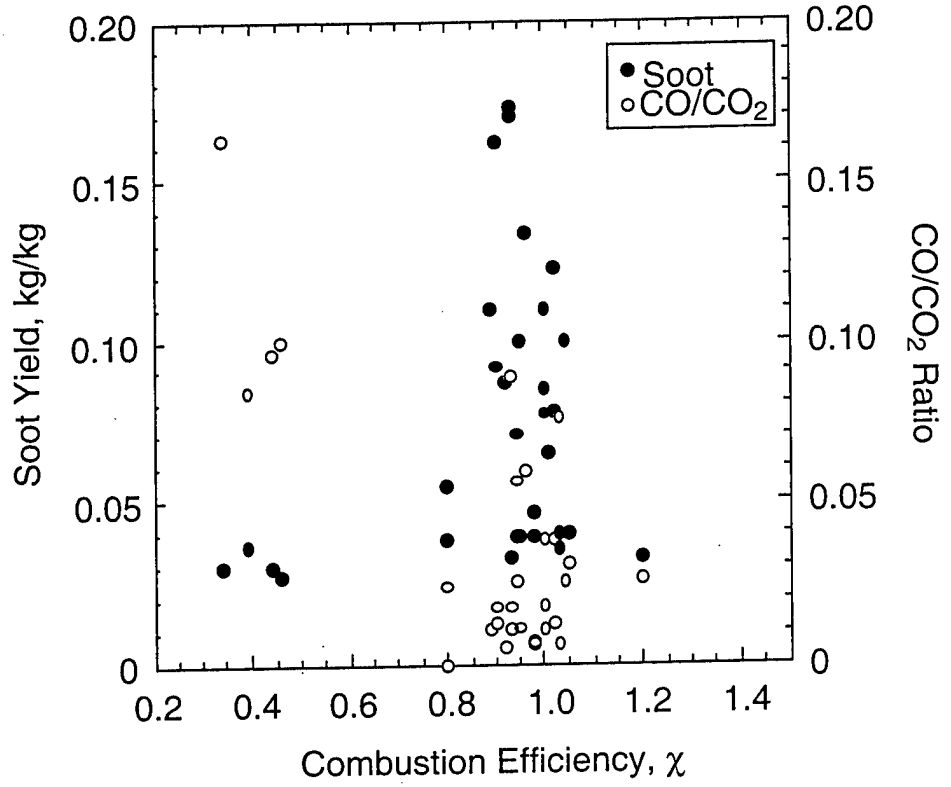

FIGURE 5. SOOT YIELD AND CO/CO_2 RATIO VERSUS COMBUSTION EFFICIENCY IN FLAME FOR CYANATE ESTERS AT IRRADIANCES TESTED IN STUDY

High soot yield and CO/CO_2 ratios are usually indicative of incomplete combustion in the flame. The data in table 5 (plotted in figure 5) show that, in general, the CO/CO_2 ratio increases as the combustion efficiency decreases as would be expected for well-ventilated flaming combustion. However, soot yield appears to be largely independent of the combustion efficiency in the flame and depends instead on the chemical structure of the polymer, being highest for the polycyanurates with pendent methyl ($-CH_3$) groups B-10, M-10, and XU-366. It is seen that χ, the soot yields, and the CO/CO_2 ratio are relatively independent of the applied external heat flux.

The high average flaming combustion efficiency for the polycyanurates calculated from all of the test data, $\chi = 0.93 \pm 0.3$, is consistent with the extremely low concentrations of hydrogen cyanide (3 ppm), carbon monoxide (207 ppm), and NO_x (3 ppm) in fire gases measured for these materials in fire calorimeters [1] and the low smoke evolution ($D_s = 1.7$) [1]. The anomalous combustion efficiencies calculated for the fluorinated cyanate ester F-10 ($\chi > 1$) suggest that the effective heat of combustion, listed in table 4, may include nonflaming heat of char oxidation (smoldering) which dominates the latter portion of the test after flame extinction.

Halogen-containing polymers usually exhibit relatively high levels of incomplete combustion products, such as CO and soot, if they burn vigorously. However, the F-10 and RD98-228 polycyanurates barely support flaming combustion, so their CO and soot yields as well as the specific extinction area for these halogen-containing polymers are comparable to, or lower than, the other polycyanurates because of the absence of gas phase combustion. The apparent

contradiction between combustion product yields and combustion efficiency for RD98-228 is in fact consistent with the thermal degradation mechanism of this polycyanurate, which produces small amounts of low- and noncombustible gases (HCl, HOCN, CO, and CO_2) and a large amount of char during pyrolysis [7]. The RD98-228 polycyanurate, when used as a matrix resin for structural composites, is the only conventionally-processed thermosetting polymer reported [22 and 23] to have passed all of the fire performance requirements for use on Navy submarines [24].

CONCLUSION

The combustibility of polycyanurates derived from a variety of cyanate ester monomers was studied in an attempt to correlate the chemical structure of these materials with their fire behavior. The effects of chemical composition were evidenced in the ignitability, burning behavior, and combustion efficiency in the flame. The halogen-containing polycyanurates were difficult to ignite and had extremely low heat release rates, while soot production and carbon monoxide yields were comparable to, or lower than, the hydrocarbon materials.

REFERENCES

1. I. Hamerton, ed., Chemistry and Technology of Cyanate Ester Resins, Blackie Academic & Professional (Chapman & Hall), London, 1994.

2. S.J. Ising and D.A. Shimp, "Flammability Resistance of Non-Brominated Cyanate Ester Resins," *Proceedings 34th International SAMPE Symposium*, pp. 1326-1334, May 8-11, 1989.

3. R.N. Walters, S. Gandhi, and R.E. Lyon, "Flammability of Cyanate Ester Resins," NIST Annual Conference on Fire Research, NIST, Gaithersburg, MD, November 2-5, 1998.

4. S. Das, D.C. Prevorsek, and B. T. DeBona, *Mod. Plast.*, 1990.

5. F.E. Arnold, J. Rodriguez-Arnold, and R. E. Lyon, "Fire Properties of a New Cyanate Ester Polymer Designed for Aircraft Applications," *4th International Fire and Materials Conference*, Crystal City, VA, November 15-17, 1995.

6. F.E. Arnold, Jr., A.M. Granville, and R.E. Lyon, "Combustion Behavior of Triazine Resins," 50th Calorimetery Conference, Gaithersburg, MD, July 23-28, 1995.

7. M. Ramirez, R.N. Walters, E.P. Savitski, and R.E. Lyon, "Thermal Decomposition of Cyanate Ester Resins," DOT/FAA/AR-01/32, FAA William J. Hughes Technical Center, September 2002.

8. ASTM Fire Test Standards, 3rd Edition, D2382-88, Standard Test Method for Heat of Combustion of Hydrocarbon Fuels by Bomb Calorimeter (High Precision Method), American Society for Testing and Materials, Philadelphia, PA, 1990.

9. V. Babrauskas, "Heat of Combustion and Potential Heat," in *Heat Release in Fires*, V. Babrauskas and S. Grayson, eds., *Elsevier Applied Science*, New York, 1992, pp. 207-223.

10. R. E. Lyon and R. N. Walters, "A Microscale Combustion Calorimeter," DOT/FAA/AR-01/117, FAA William J. Hughes Technical Center, February 2002.

11. W.M. Thornton, *Philos. Mag.* 33, 196, 1917.

12. C. Hugget, "Estimation of Rate of Heat Release by Means of Oxygen Consumption Measurements," Center for Fire Research, National Bureau of Standards, Washington, DC 20234, *Fire and Materials*, 4 (2), 1980.

13. R.N. Walters and R. E. Lyon, "A Microscale Combustion Calorimeter for Determining Flammability Parameters of Materials," *Proceedings 42nd International SAMPE Symposium and Exhibition*, 42(2), 1335-1344, 1997.

14. R.N. Walters and R.E. Lyon, "Molar Group Contributions to Polymer Flammability," *Proceedings ACS National Meeting, Fire and Polymers Symposium*, Washington, DC, August 20-24, 2000.

15. ASTM E1354, "Standard Test Method for Heat and Visible Smoke Release Rates for Materials and Products Using the Oxygen Consumption Calorimeter," American Society for Testing and Materials, Philadelphia, PA, 1995.

16. V. Babrauskas, "Development of Cone Calorimeter - A Bench-Scale Heat Release Apparatus Based on Oxygen Consumption," *J. Fire Science*, 2, 81, 1984.

17. D.W. Van Krevelen, "Properties of Polymers," Third Edition, pp. 649-652, *Elsevier Science*, The Netherlands, 1990.

18. A. Tewarson, in SFPE Handbook of Fire Protection Engineering, 2nd Edition, Chapters 3-4, "Generation of Heat and Chemical Compounds in Fires," Society of Fire Protection Engineers, Boston, MA, 1995.

19. J.G. Quintiere and Harkleroad, M., "New Concepts for Measuring Flame Spread Properties," NBSIR 84-2943, 1984.

20. W.J. Parker, "Development of a Model for the Heat Release Rate of Wood," NBISR 85-3163, 1985.

21. R.E. Lyon, "Solid State Thermochemistry of Flaming Combustion," in *Fire Retardancy of Polymeric Materials*, A.F Grand and C.A. Wilkie, (eds.), Marcel Dekker, Inc., NY, pp. 391-447, 2000.

22. J. Koo, B. Muskopf, G. McCord, P. VanDine, B. Spencer, U. Sorathia, and S. Venumbaka, "Characterization of Fire Safe Polymer Matrix Composites for Naval Applications," *Proceedings 46th International SAMPE Symposium & Exhibition*, Long Beach, CA, May 6-10, 2001.

23. P. VanDine and U. Sorathia, "Developments in Fire Proof Composites," *Proceedings 46th International SAMPE Symposium & Exhibition*, Long Beach, CA, May 6-10, 2001.

24. MIL-STD-2031, "Fire and Toxicity Test Methods and Qualification Procedure for Composite Materials Systems Used in Hull, Machinery, and Structural Applications Inside Naval Submarines," 1991.

APPENDIX A—HEAT RELEASE HISTORIES OF POLYCYANURATES AT INDICATED HEAT FLUXES

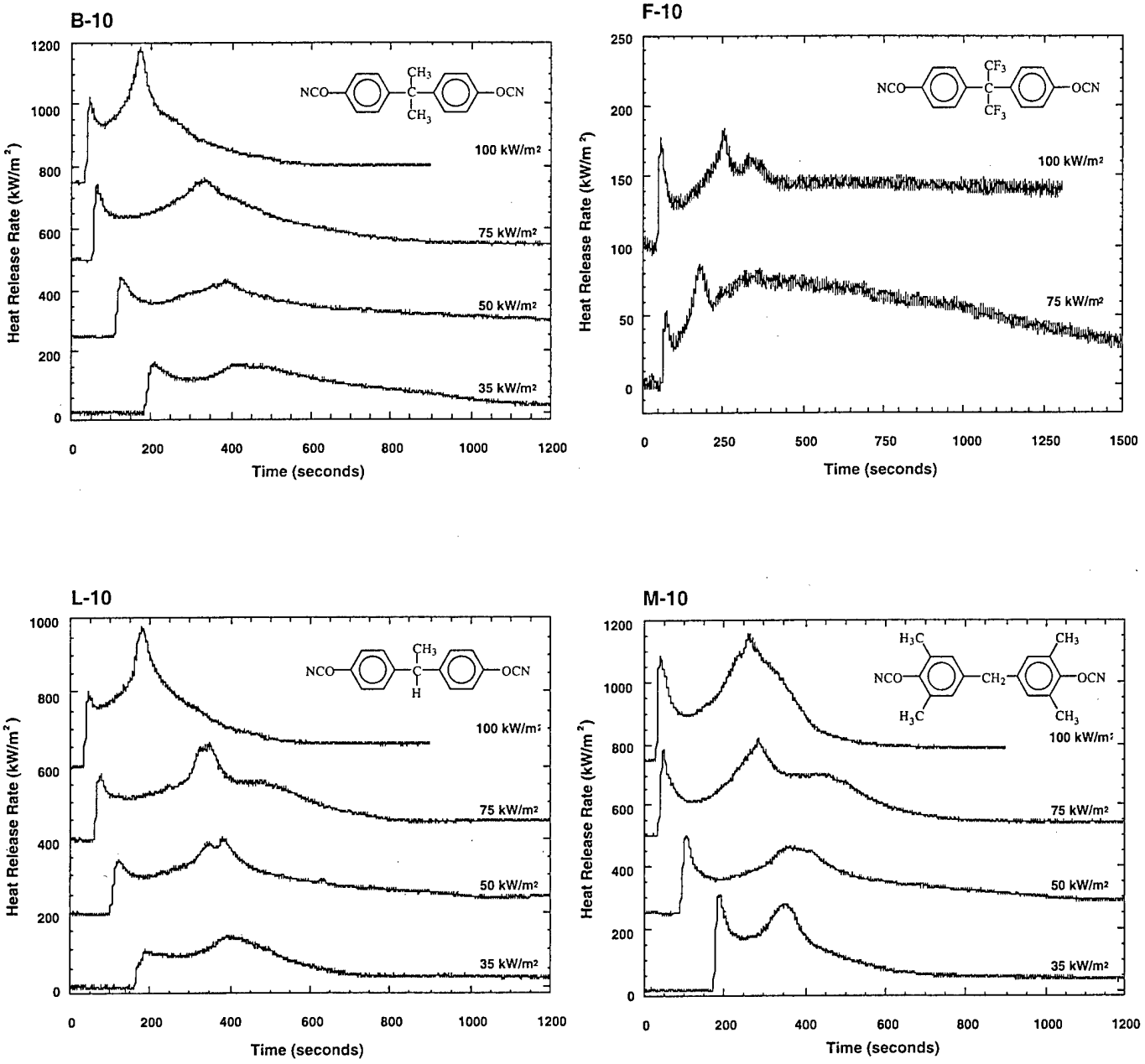

FIGURE A-1. HEAT RELEASE RATE HISTORIES FOR B-10, F-10, L-10 AND M-10 POLYCYANURATES AT INDICATED HEAT FLUXES

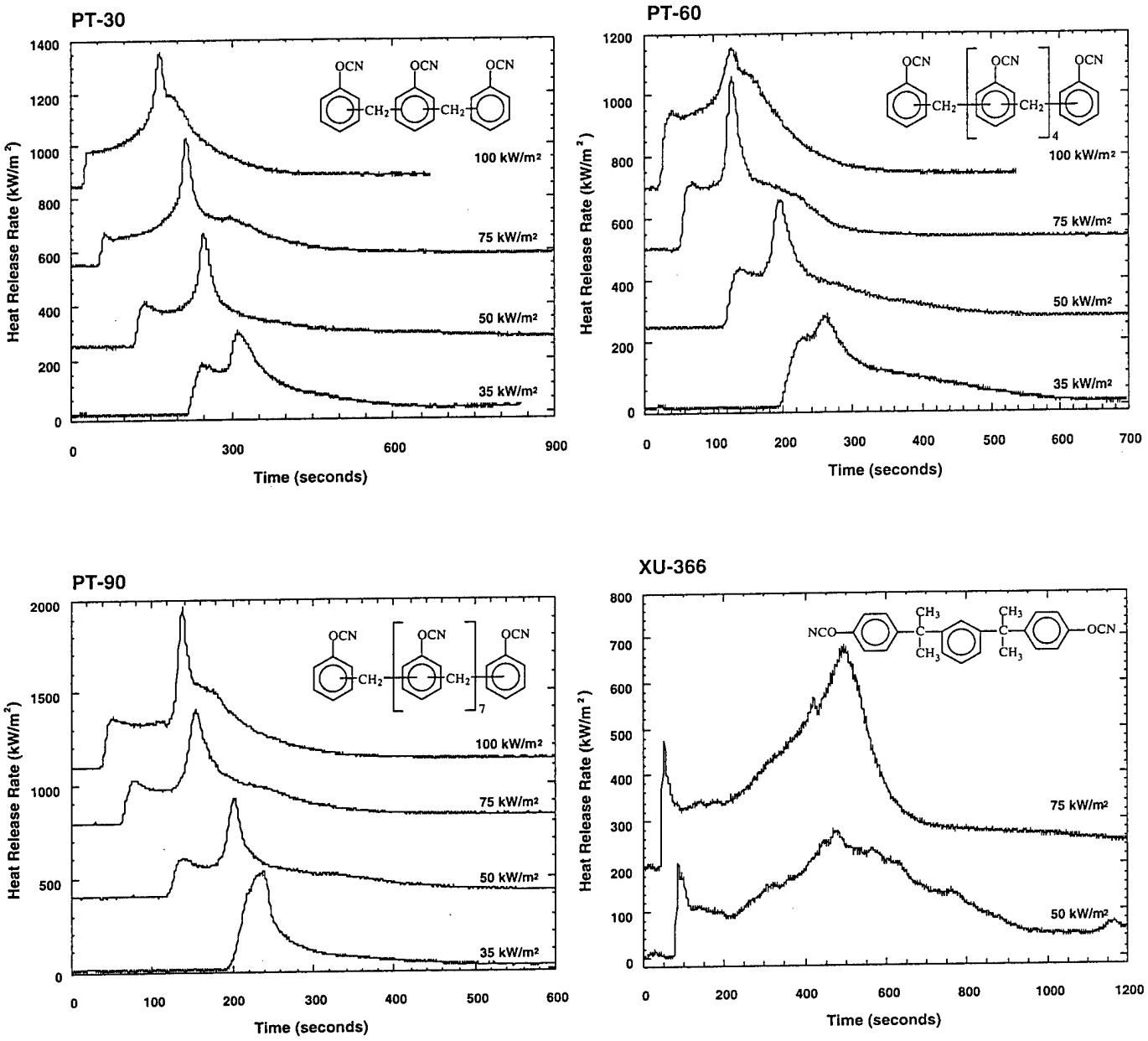

FIGURE A-2. HEAT RELEASE RATE HISTORIES FOR PT-30, PT-60, PT-90, AND XU-366 POLYCYANURATES AT INDICATED HEAT FLUXES

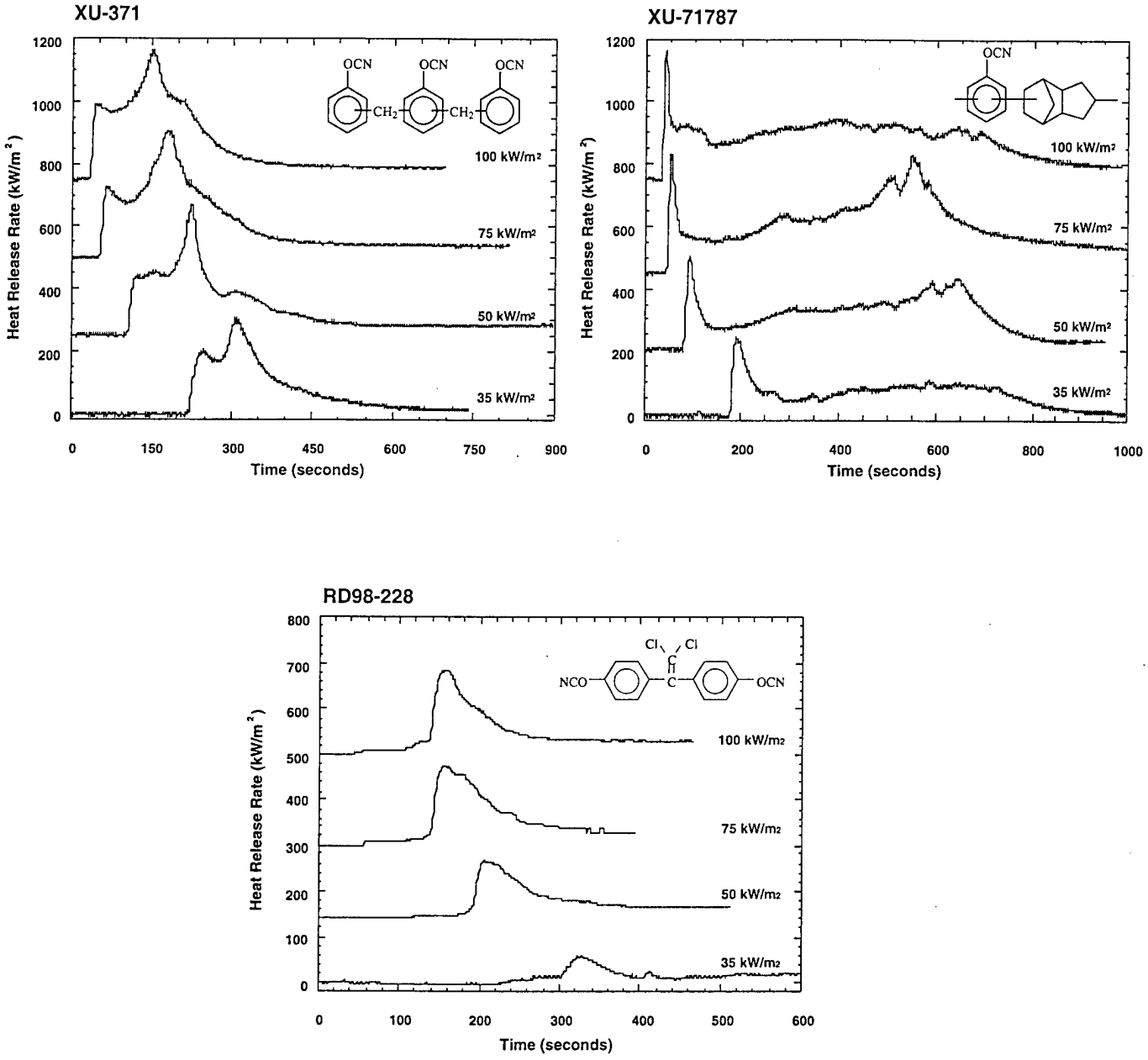

FIGURE A-3. HEAT RELEASE RATE HISTORIES FOR XU-371, XU-71787, AND RD98-228 POLYCYANURATES AT INDICATED HEAT FLUXES